$Ti_3C_2T_x$ MXene as Surface-Enhanced Raman Scattering Substrate

Hayk Minassian*[1], Armen Melikyan[2], Manuel Rodrigues Goncalves*[3] and Petros Petrosyan[4]

[1]A. Alikhanian National Science Laboratory, Alikhanyan Str. Build. 2, 0036, Yerevan, Armenia

[2] Institute of Applied Problems of Physics of NAS, 25, Hr.Nersessian Str., 0014, Yerevan, Armenia

[3]Ulm University - Institute of Experimental Physics, Albert-Einstein-Allee 11, 89081 Ulm, Germany

[4]Yerevan State University, 1 Alek Manukyan St, 0025, Yerevan, Armenia

* Correspondence: hminassian@yerphi.am, manuel.goncalves@uni-ulm.de

Supporting Information (SI)

SI-Table 1. Measured values of EFs in different MXenes and excitation wavelengths

MXene substrate	**SERS enhancement factor**	**Laser wavelength (nm)**	**Ref.**
$Ti_3C_2T_x$ (in solution and on glass)	10^5 - 10^6	488 nm, 514nm	[18]
Freestanding $Ti_3C_2T_x$ membrane	10^6	532 nm	[20]

Crystalline monolayer Ti_3C_2	3.82×10^8	532	[23]
$Ti_3C_2T_x$ on glass	220	532, 633, 785	[24]
Nb_2C and Ta_2C	3.0×10^6 and 1.4×10^6	532	[25]
Mo_2C, Ti_2C, V_2C, Mo_2TiC_2, and Ti_3CN	10^5 - 10^6	488, 514, 633, and 785	[26]

SI-2. Modelling of the R6G molecule

We proceed with the formula that expresses the relation of ACS of the dye molecule $\sigma_{\mathrm{R6G}}(\lambda)$ and the imaginary part of polarizability $\alpha_{\mathrm{R6G}}(\lambda)$ of R6G [S1].

$$\sigma_{\mathrm{R6G}}(\lambda)=\frac{8\pi^2}{\lambda}\Im\left[\alpha_{\mathrm{R6G}}(\lambda)\right] \qquad \text{(SI 1.1)}$$

We exploit experimental data of ACS for R6G molecule on glass substrate and in water [32-34] to calculate $\Im\left[\alpha_{\mathrm{R6G}}(\lambda)\right]$ from (SI1.1). The real part of polarizability is taken from [34, 35] where $\Re\left[\alpha_{\mathrm{R6G}}(\lambda)\right]$ is calculated using the Kramers-Kronig relation. Thus, the complex polarizability of R6G is obtained based on these two functions. Moreover, a random orientation of the dye in water, or on a substrate, suggests to consider the R6G molecule as a small sphere of radius $R \ll \lambda$. Applying the well-known expression for $\alpha_{\mathrm{R6G}}(\lambda)$ in the quasi-static approximation [S2]

$$\alpha(\lambda)=\frac{\epsilon_{\mathrm{R6G}}(\lambda)-\epsilon_M}{\epsilon_{\mathrm{R6G}}(\lambda)+2\,\epsilon_M}\cdot R^3 \qquad \text{(SI 1.2)}$$

where ϵ_M is the dielectric constant of the surrounding medium, we find the complex dielectric function $\epsilon_{\mathrm{R6G}}(\lambda)$ of R6G solving the inverse problem from (SI 1.2). Namely, having measured $\alpha(\lambda)$, we find $\epsilon_{\mathrm{R6G}}(\lambda)$ from (SI 1.2) employing R as a fitting parameter. The wavelength dependent ACS of the dye molecule is calculated using $\epsilon_{\mathrm{R6G}}(\lambda)$ in COMSOL Multiphysics. Thus, we find the fitting value of the parameter R that achieves a good overlapping between the calculated ACS spectrum and the maximum values of experimental data. The present method gives, for the case of glass substrate ($\lambda_{\text{res}} = 545\,\text{nm}$) [32]) and water [34]) the following values for the auxiliary parameter $R = 0.31\,\text{nm}$ and $R = 0.27\,\text{nm}$, respectively.

The result of the simulation corresponding to found value of R is presented in Fig. SI-1 a) and b) which demonstrates good matching with the experimental data.

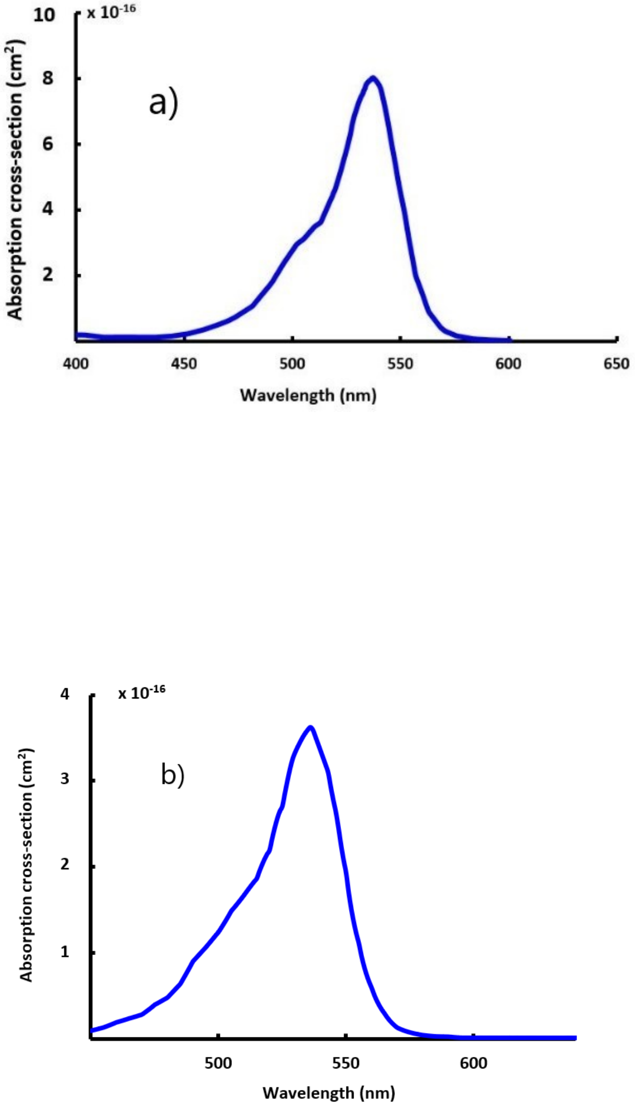

Figure SI-2. Calculated ACS of R6G molecule modeled as a spherical particle, on a glass substrate (a) and in water (b).

SI-3. Surface charge distribution map at wavelengths

COMSOL simulations show that for a NE with long axis of $2a = 500\,\text{nm}$, at $\lambda \geq 2250\,\text{nm}$ there appear only longitudinal dipole oscillations. The corresponding surface charge distribution is presented in the Fig. SI-3. It is evident that higher multipole modes are not present.

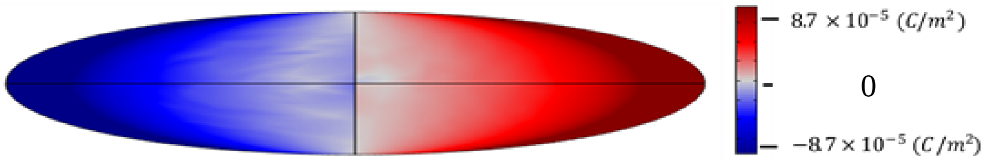

Figure SI-3. Surface charge distribution map in NE ($2a=500\,\mathrm{nm}$) at $\lambda=2250\,\mathrm{nm}$, when the incident light is polarized along the large axis of NE.

SI-4. Dispersion of refractive index

To assess the role of larger particles in SERS we present the dispersion of refractive index of a $400\,\mathrm{nm}$ thick MXene flake using the experimental data of the dielectric function [15].

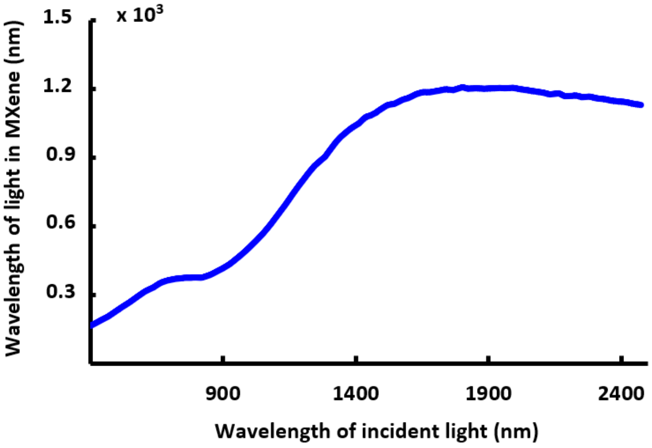

Figure SI-4. Incident light wavelength in MXene.

For long wavelengths, $\lambda \leq 2400\,\mathrm{nm}$, the light wavelength in the flake is notably small compared to the vacuum wavelength of the incident light. This is the reason for larger NPs with LQSP and TQSP modes to contribute more to SERS than IBT.

SI-5. Absorption cross-section and SERS EF dependence on wavelength for the NE with $2a=1000\,\mathrm{nm}$ and NR of length $l=1000\,\mathrm{nm}$ on glass substrate.

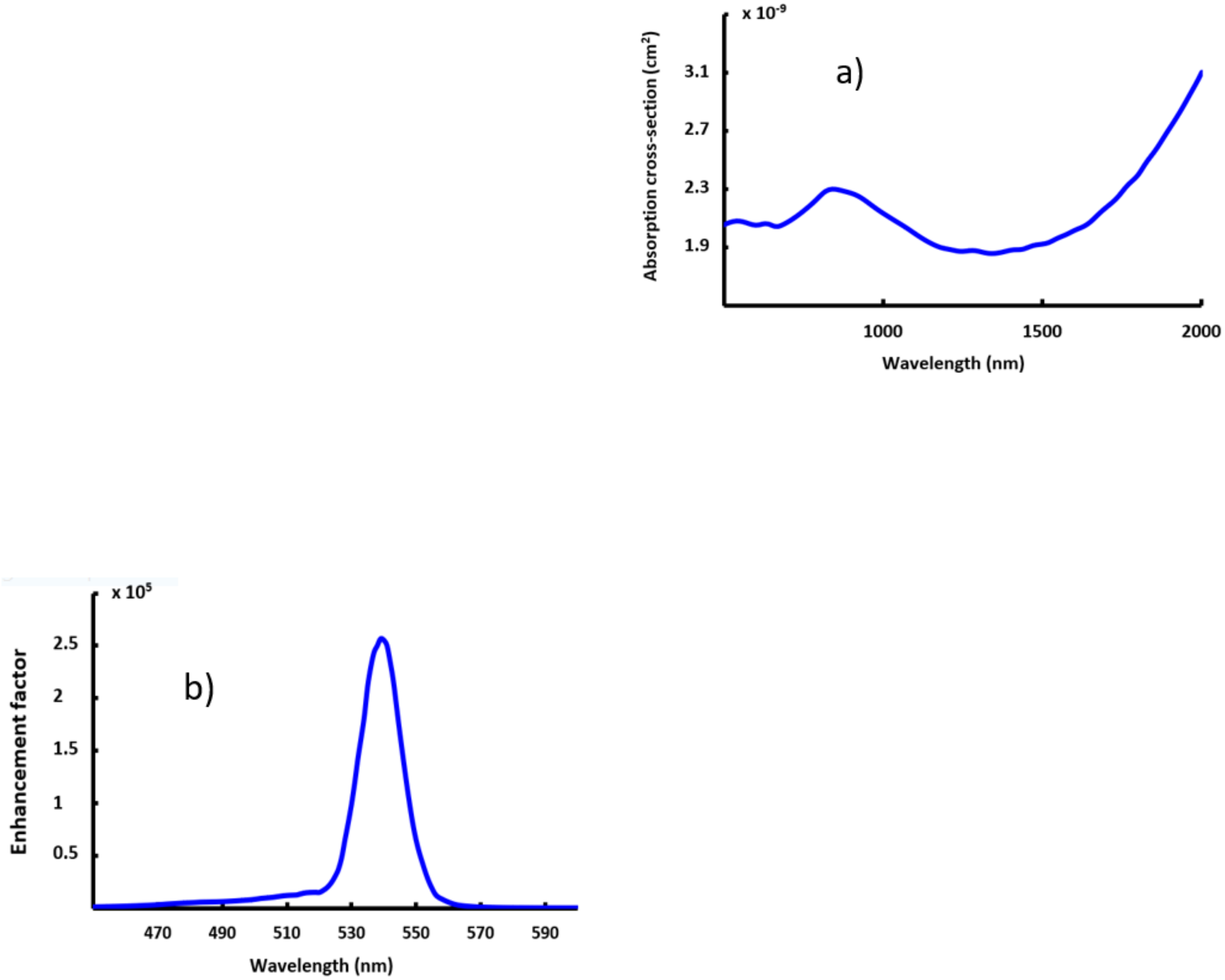

Figure SI-5-1. Absorption cross-section (a) and EF (b) dependence on the wavelength in a system composed by a spherical R6G molecule and a MXene NE with $2a=1000\,\mathrm{nm}$ and aspect ratios $\eta_1 \approx 3$ and $\eta_2 \approx 15$ on glass substrate.

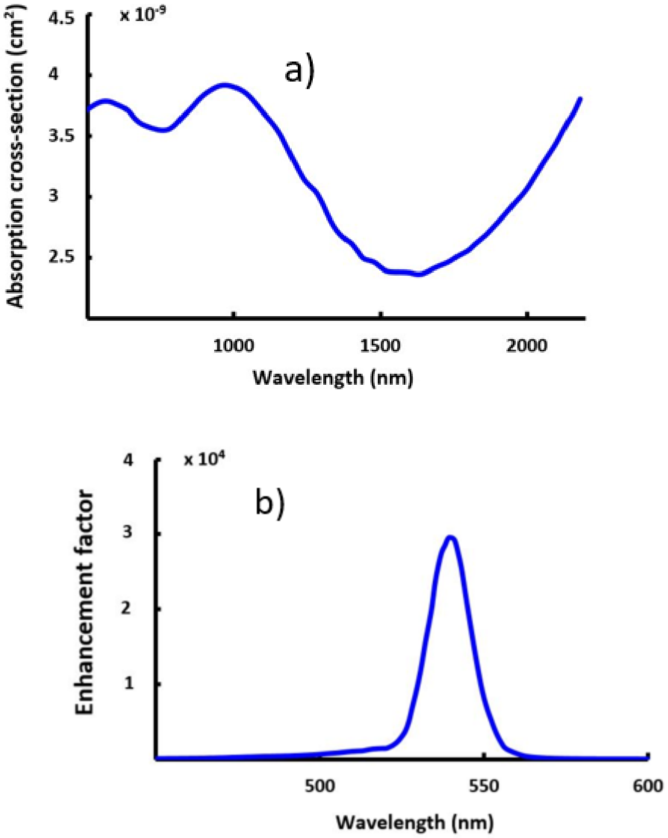

Figure SI-5-2. a) Absorption cross-section (a) and EF (b) dependence on the wavelength in the system of a spherical R6G molecule and a MXene NR with $l = 1000\,\mathrm{nm}$ and diameter $d = 347\,\mathrm{nm}$ on glass substrate.

SI-6. Charge distribution maps of large $Ti_3C_2T_x$ NEs.

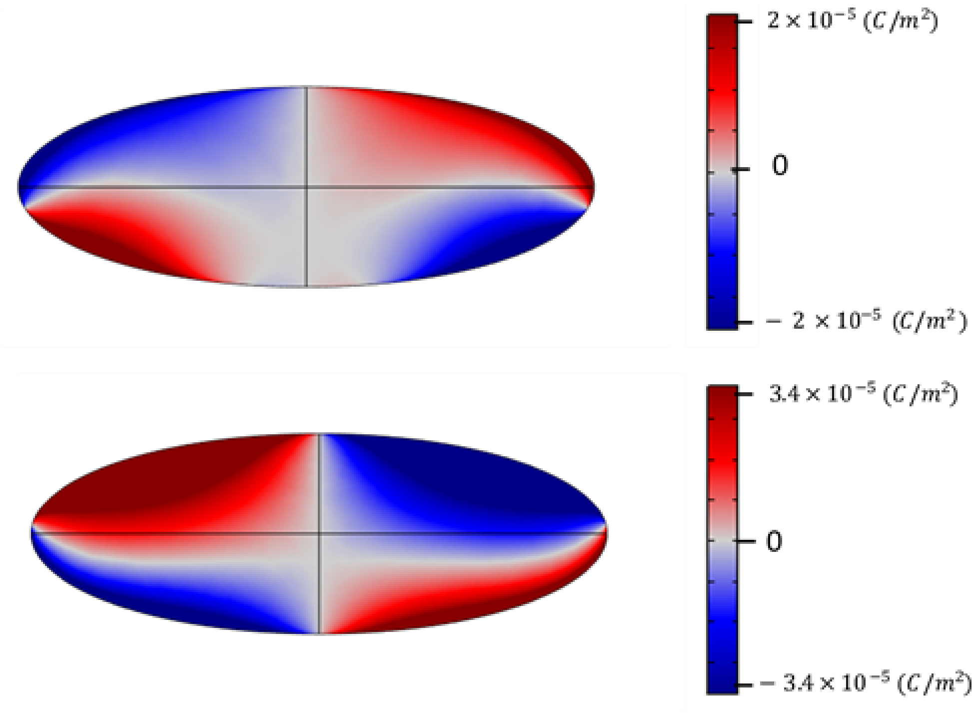

Figure SI-6-1. Surface charge distribution map of a NE with $2a = 1500\,\mathrm{nm}$ at two maxima - $\lambda = 960\,\mathrm{nm}$ and $\lambda = 1540\,\mathrm{nm}$. The incident electric field is directed along NE long axis.

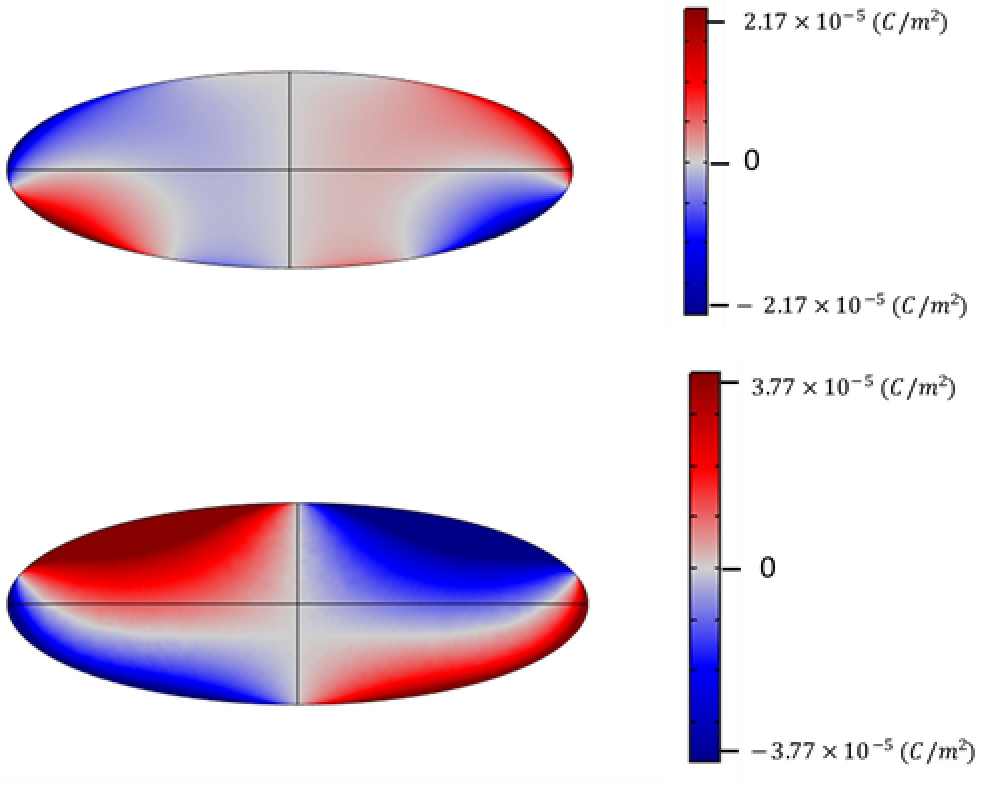

Figure SI-6-2. Surface charge distribution map of a NE with $2a = 2000\,\mathrm{nm}$ at two maxima $\lambda = 1000\,\mathrm{nm}$ and $\lambda = 1830\,\mathrm{nm}$.

SI-7. Charge and field distribution maps of the NE dimer

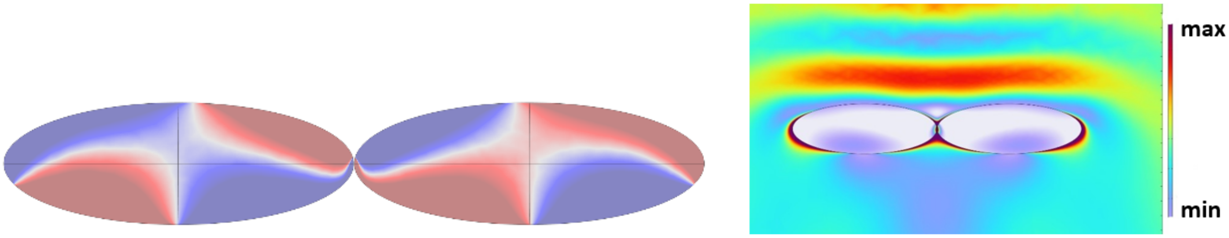

Figure SI-7. Surface charge distribution map in NE ($2a = 1000\,\mathrm{nm}$ and aspect ratios $\eta_1 \approx 3$, $\eta_2 \approx 15$) at $\lambda = 960\,\mathrm{nm}$, when the incident light is polarized along the longest axis.

SI-8. Analytical calculation of the SERS EF in small MXene flakes based on the quasi-static approximation.

We consider a R6G molecule placed near the $Ti_3C_2T_x$ flake in the form of NS with linear sizes much smaller than the wavelength λ, which allows us to apply the quasi-static approximation for electromagnetic fields. The problem of SERS by a small molecule of constant polarizability in the vicinity of a metallic half spheroid was solved analytically for the first time in [3]. We consider the dye molecule approximated as a point dipole with frequency dependent polarizability $\alpha(\omega)$ near the small MXene spheroid with known dielectric function $\epsilon(\omega)$ (see references [5,14] of the article). Following the method developed in [3] we obtain the EF from (1) following the expression in the quasi-static approximation

$$G=\left|\frac{\dfrac{\epsilon(\omega)}{[\epsilon(\omega)-1]L_1(\xi)+1}}{1-\dfrac{\epsilon(\omega)-1}{\epsilon(\omega)+1}\cdot\dfrac{2-y+y^2}{8h^3}\cdot\alpha(\omega)}\right|^4 \qquad \text{(SI 8-1)}$$

where $L_1(\xi)=(\xi^2-1)\cdot\left[\frac{\xi}{2}\ln\left(\frac{\xi+1}{\xi-1}\right)-1\right]$, $\xi=\sqrt{c^2/(c^2-a^2)}$, c and a are the major and the minor semiaxes of the NS, $y=h/\rho$, h is a distance between the apex of the spheroid and the point dipole. y is much smaller than the radius of curvature at the vertex ρ of the spheroid . The multiplier $(2-y+y^2)$ in the denominator of SI 8.1 accounts approximately for the curvature. When $y=0$ we have the case of a molecule near an infinite plane.

The numerator in SI 8-1 is the electric field created by the spheroid, polarized by the incident wave (i.e. excluding the reaction field) at the point close to apex and normalized to the amplitude of the incident field. Thus, it describes the following EM mechanisms of enhancement - the lightning-rod and the polarization induced by IBT. The image effect is described by the reciprocal of denominator of SI 8-1, since it includes the contribution of the reaction field, denoted by y. Since in the vis-NIR range considered there are no dipole SP resonances, the SERS EF is determined by the image and the lightning-rod effects, being the latter enhanced by IBT.

It turns out that, it is possible to change the geometry of the system (single spheroidal flake of $Ti_3C_2T_x$ and dye molecule) to bring closer the resonances corresponding to the lightening-rod and molecular absorption. The corresponding optimization of the EF for a small spheroidal nanoparticle with major and minor semiaxes of $30\,\mathrm{nm}$ and $5\,\mathrm{nm}$ (the curvature radius is $1.629\,\mathrm{nm}$) gives the following value for the distance $h=0.565\,\mathrm{nm}$. In Figure SI-8 (blue line) we present the plot of wavelength dependence of EF for this particular case. The optimized value of the EF in the visible range varies from 0.5×10^6 to 1.1×10^6. Since the expression SI 8-1 allows to separate the contributions of the lightning-rod and the image effects, we present in Figure SI-8 the contributions due to these two mechanisms (in green and red, respectively). As it follows from the expression SI 8-1, the total EF is a product of these two contributions for any λ. We note that the contribution of image effect to the SERS EF is much weaker than that produced by the lightning-rod effect.

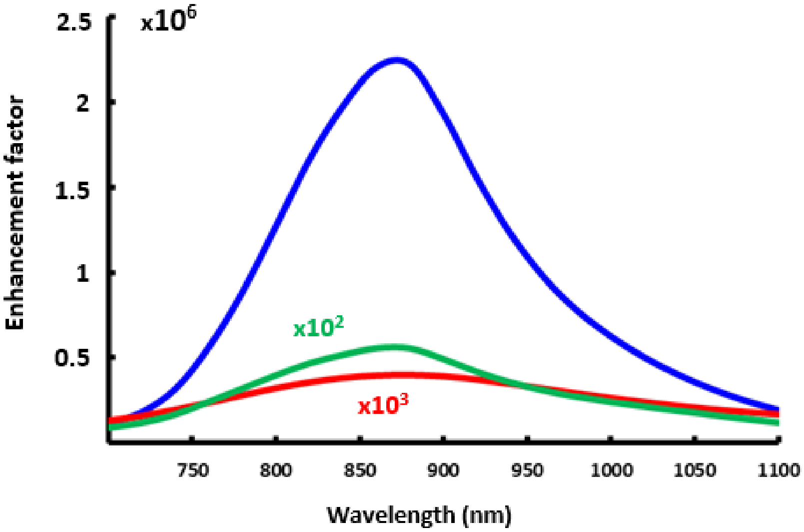

Figure SI-8. Wavelength dependence of SERS EF of R6G molecule near the $Ti_3C_2T_x$ nanospheroid (NS) with semiaxes $30\,\mathrm{nm}$ and $5\,\mathrm{nm}$ in vacuum (blue). Separate contributions into EF corresponding to the lightning rod (green) and image effects (red) are presented. The separation between the R6G molecule and the NS apex is $h=0.565\,\mathrm{nm}$.

References

S1. J. D. Jackson, Classical electrodynamics, John Wiley & Sons, Inc. 1999.

S2. V. Klimov, Nano Plasmonics, Taylor & Francis 2013.

S3. Gersten, A; Nitzan. A. Electromagnetic theory of enhanced Raman scattering by molecules adsorbed on rough surfaces. J. Chem. Phys. 73, **1980**, 3023-3037. doi:10.1063/1.440560.